Chemical Applications of a Programmable Image Acquisition System (submitted to *J. Chem. Educ*. 07/27/01)

Paul J. Ogren, Ian Henry, and Steven E.S. Fletcher
Chemistry Department, Earlham College, Richmond, IN 47374 paulo@earlham.edu

Introduction

Many important chemical techniques rely upon visual imagery, from paper and thin-layer chromatography, to dye-treated electrophoresis gels, to kinetic systems involving changes in colors and patterns. Spectrophotometry and densitometry are commonly used to quantify such images, and dedicated commercial instrumentation is often available for particular methods. We describe a cost-effective and versatile system consisting of a CCD camera, video acquisition board, and a flexible programming environment which can be used for all of these applications. We present overviews of five examples and note some special considerations for data collection and processing. In addition to these illustrations, which may be used with a number of experiments in organic, analytical, physical, or biochemistry, the system provides many opportunities for small student projects in further software developments and applications. For example, the camera and software options are quite suitable for the analysis of still or time-dependent images in optical microscopy, and the software itself is suitable for the processing of images in a large range of standard formats.

The system depicted in Figure 1 uses National Instruments IMAQ and LabVIEW software *(1,2),* a SONY machine-vision XC-73 monochrome camera, a National Instruments PCI 1407 video board, and a Gateway 800 MHz computer system. Light sources consist of light boxes for transmission images, standard floodlights for reflected images, or UV sources commonly used for fluorescence detection in chromatography. Optical filtering is used as needed. We use several LabVIEW stations in our laboratory program, and a ten-user license for the IMAQ imaging software is an additional $1500. The cost of the camera system and video board for one station is about $1750. Further details are available in the *JCE Online* supplemental material.

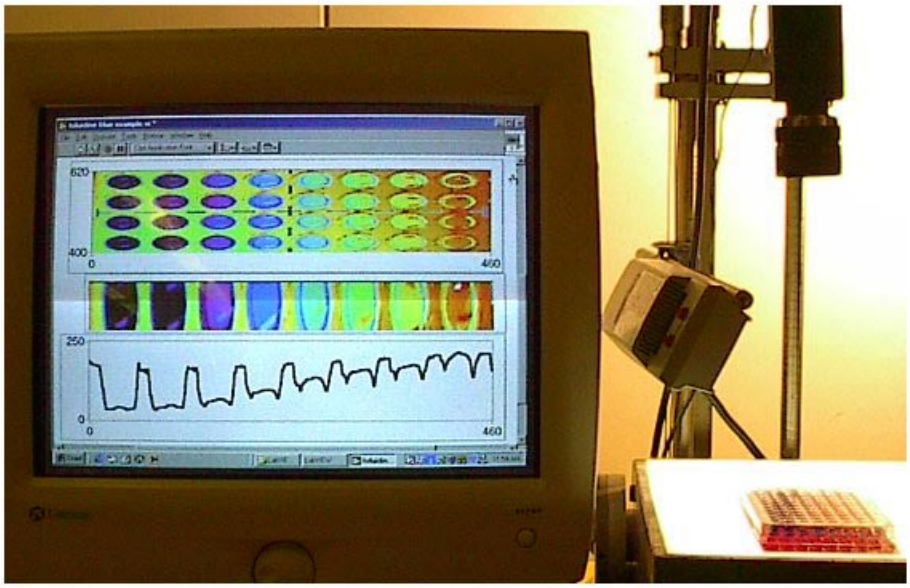

Figure 1. The arrangement of the system for well plate acquisition and analysis. The upper part of the computer screen displays a processed image of four rows containing duplicate sets of toluidine blue aqueous solutions (λ_{max} = 633 nm). The original image is a standard 9 x 12 well plate. The light box source (I^2R, Inc.) is filtered by a Rosco #43 plastic sheet (λ_{max} = 680 nm, bandwidth ca. 80 nm, Edmund Scientific). In normal operations, the tilted UV source (UVG Inc. model UVGL-25), CCD camera, light box, and sample are enclosed in a black plywood box to minimize stray light sources.

Example 1: Well plate analyses

Well plate measurements are used for rapid colorimetric analyses, including immunoassays such as ELISA *(3,4 pp. 279-289).* The toluidine blue solution concentrations in Figure 1 decrease from 2 x 10^{-4} M by factors of two, with the right well in the image being the blank. Identical volumes are in each well, and sample depths are about 3 mm. The lowest of the four displayed rows is magnified and cropped in the middle part of the computer screen image. The measured signals at each pixel are averaged over the vertical direction (y) of this magnified image, and the results are shown in the lower graph. The centers of the signal dips for each well in the cropped image measure the light transmitted through each solution. The data for the lower graph is also transferred to a spreadsheet which is then used to create the calibration graph shown in Figure 2. The standard Beer's Law plot is not linear at higher concentrations because the requirement of narrow source bandwidth does not fully apply. The IMAQ software options for recognition and alignment of patterns such as a well plate image also provide possibilities for the rapid analysis of batches of well plate results.

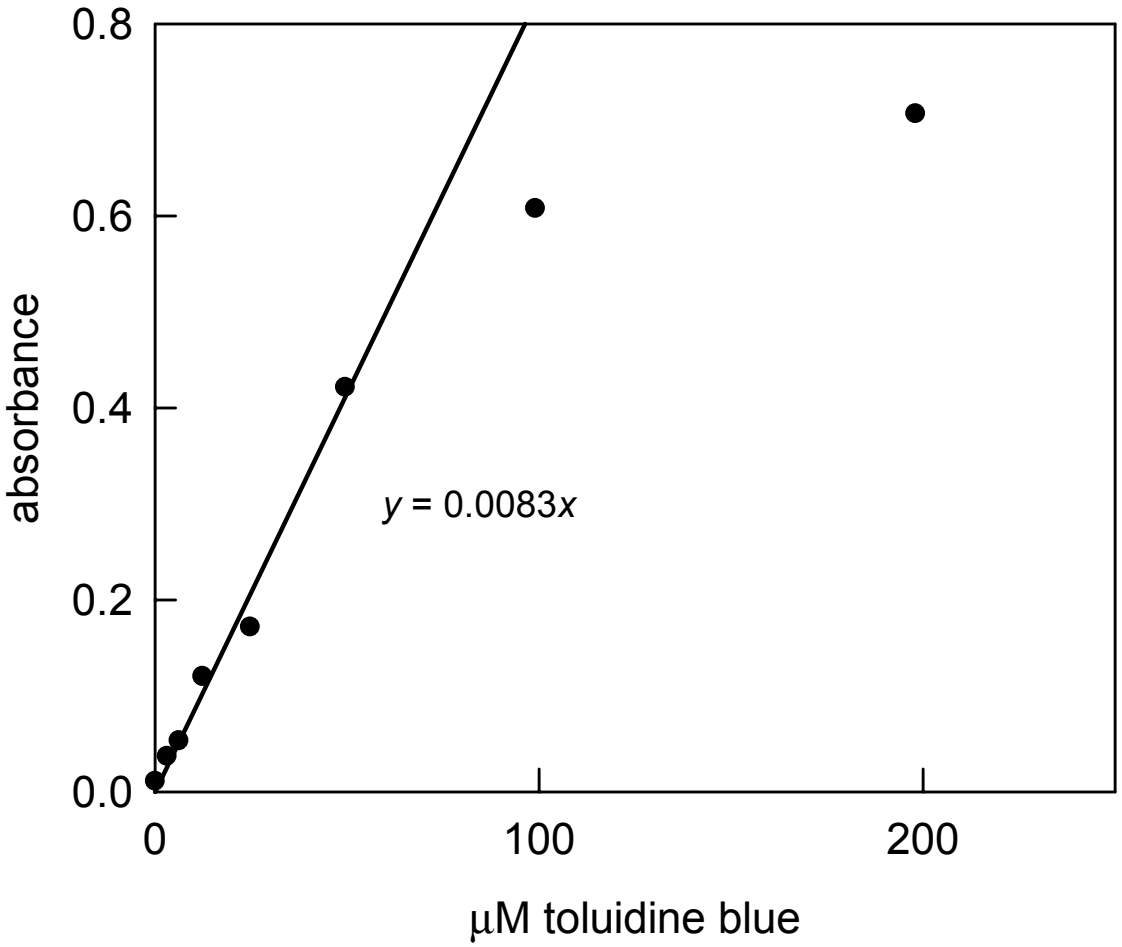

Figure 2. Beer's Law plot of the Figure 1 well plate data. The blank transmission for each well i is measured by averaging transmission signals on each side of the well, and Excel is used to calculate absorbances from transmissions given by $T(i) = well\ signal(i) / blank(i)$. Linearity is good below an absorbance of about 0.5.

Example 2: TLC quantitative analysis of acetaminophen and aspirin

Extraction followed by thin layer chromatography and fluorescence detection of compounds in commercial drugs is a standard early organic experiment *(5)*. The usual goal is to identify compounds by comparative R_f values, and to make semi-quantitative visual estimates of amounts by comparison with known standards. This example demonstrates the feasibility of a much more quantitative evaluation of TLC images. The "hand-held" UV excitation source shown in Figure 1 is typical of those used in this type of experiment, and has been adapted for fixed mounting in our system. Figure 3 shows the image of a fluorescing TLC plate with acetaminophen and aspirin standards, and extracts from two commercial tablets. The two rightmost samples in the image are from a 325 mg aspirin tablet and a 325 mg Tylenol tablet (each tablet crushed and extracted with 100 mL 50:50 ethanol:methylene chloride, 3 applications to the TLC plate). The other samples are from 1, 2, 4 and 6 applications of a standard containing 50 mg of each compound in 20 mL of the ethanol:methylene chloride solvent. The same capillary was used to apply all of the samples to the TLC plate. The eluent is 50:50 hexane:ethyl acetate containing 3% glacial acetic acid.

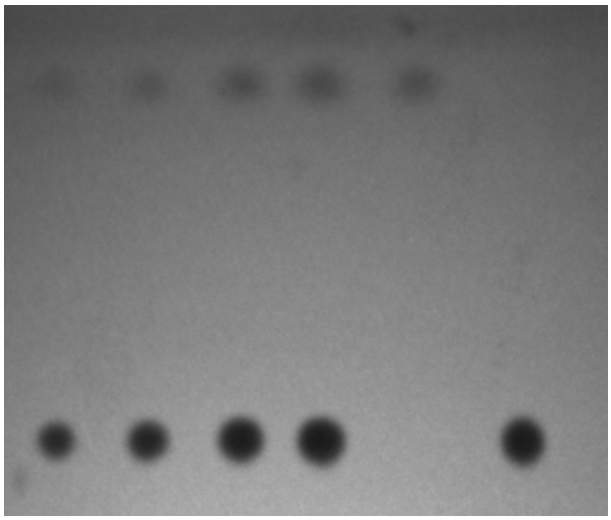

Figure 3. This camera image of fluorescence from a 5 cm x 5 cm region of a TLC plate shows six samples of acetaminophen (lower spots) and acetylsalicylic acid (upper spots). The starting points are just below the displayed image region. The camera f-stop is used to set the maximum recorded intensity to about 240 units (saturation is 256). The UV excitation is primarily at 254 nm.

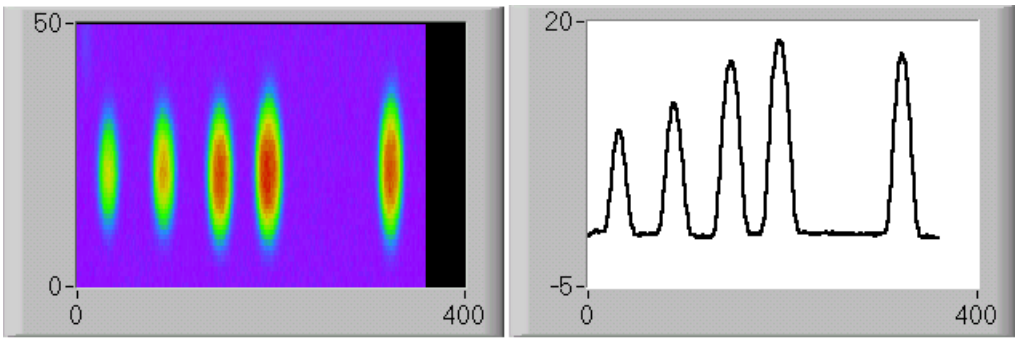

Figure 4. The user selects suitable regions for detailed analysis, as shown in this LabVIEW panel display of the acetaminophen spots of Figure 3. The graph on the left displays absorbances using a color ramp to depict intensity variations in the original panel (the original purple background shows as dark gray in this figure). The graph on the right depicts absorbance sums in the vertical (y) direction as a function of pixel positions in the x direction. The gap occurs for the aspirin sample, and the rightmost peak in the sequence is for Tylenol.

The LabVIEW panel of Figure 4 shows UV absorbance contours[1] for the acetaminophen spots and a plot of the pixel absorbance sums for vertical slices through the image. Data points for this graph are stored in Excel, which is then used to determine areas under the peaks. This gives total absorbance sums for each spot, and these are used to give the calibration line of Figure 5. Repeated trials with standards show that the slight curvature of the data is typical for samples with relatively high absorbances. The time required for students to obtain results typified by Figure 4 is about 5 minutes.

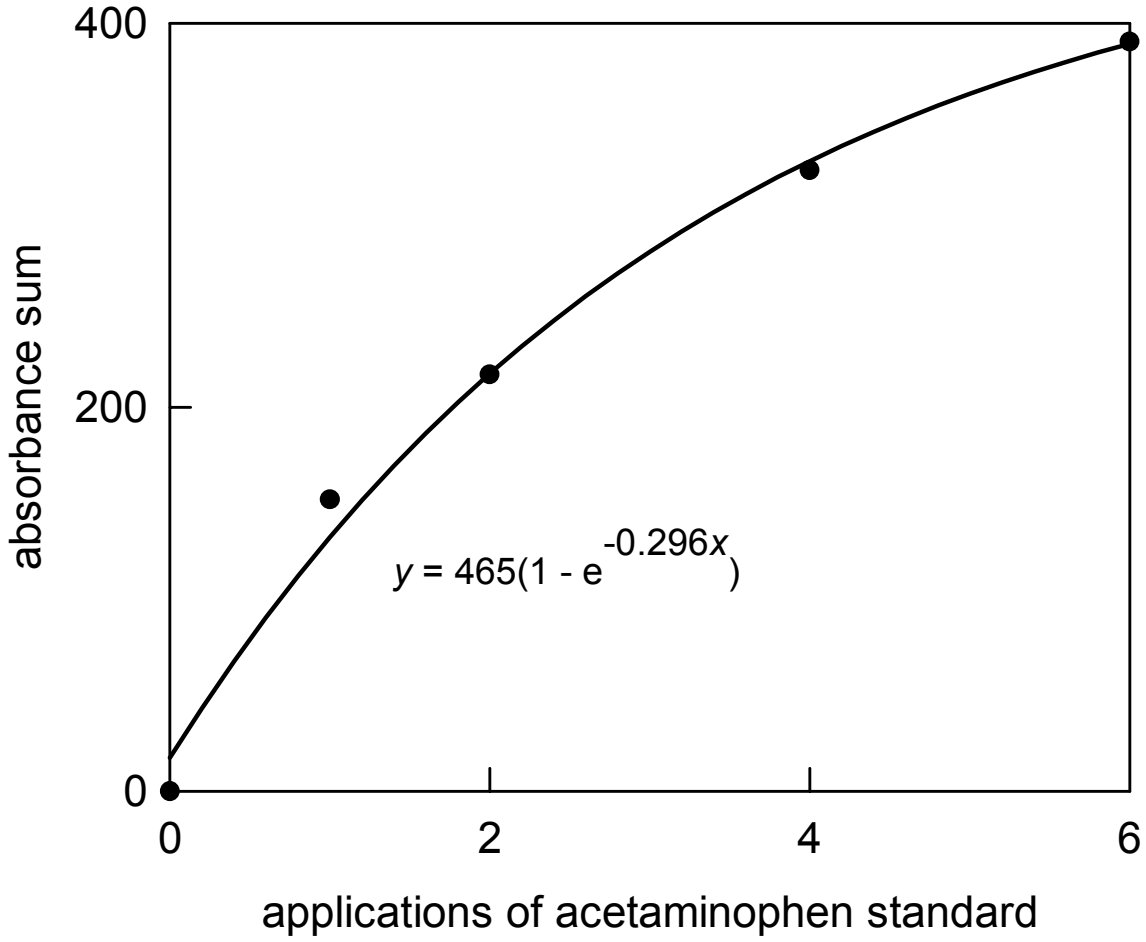

Figure 5. A standard curve for the acetaminophen data of Figure 4. This curve gives a value of 335 mg ± 8% for the Tylenol tablet (the bottle label states 325 mg acetaminophen).

Example 3: Analysis of electrophoresis bands

Electrophoresis is a standard method in biochemistry for the study of DNA and protein molecules. Figure 6 shows the camera image of a DNA electrophoresis gel *(4, pp. 61-77)*. Lanes 3, 7 and 11 contain a DNA ladder standard at different concentrations, and lanes 5 and 9 contain single purified experimental samples. The program of the preceding example extracts "densitometry" information along selected lanes, leading to the plots of Figures 7 and 8. Figure 7 is a standard calibration which can be used to determine the base pair (bp) numbers of other samples in adjacent lanes, and Figure 8 shows that the relationships between integrated peak intensities and amounts of the

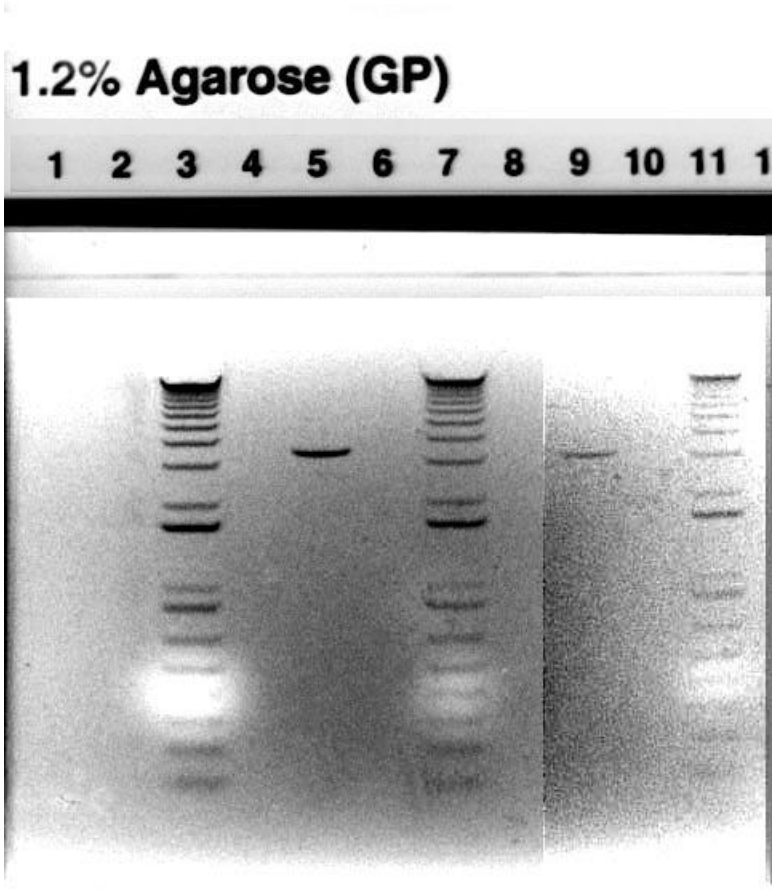

Figure 6. In this "negative", fluorescence of DNA-bound ethidium bromide marks the presence of fragments of different sizes. The DNA standards in lanes 3, 7 and 11 also contain methylene blue as a visual indicator, and this shows up as light spots in the image near the 500 bp region. Fluorescence is excited with a 312 nm UV source and the resulting orange emission passes through a Kodak Wratten 22 filter cutting off wavelengths below 550 nm. Separate contrast factors have been used in the 1 – 8 and the 9 – 11 lane regions to maximize visual clarity.

standards can be used to establish standard curves for the quantitation of similar fragments. For the "unknown" fragment in lane 9, the Figure 7 results predict a size of 3120 (± 60) bp. The signal sum for this fragment is 1060, corresponding to 7.7 ng of material from the Figure 8 results. The calculation of the amount of material assumes a constant UV excitation background. Furthermore, the ethidium bromide in the gel migrates to some extent during electrophoresis, and the amount of binding to DNA must be dependent on fragment size. Because of these factors, comparisons of unknowns with standards must be made at similar migration positions in the gel.

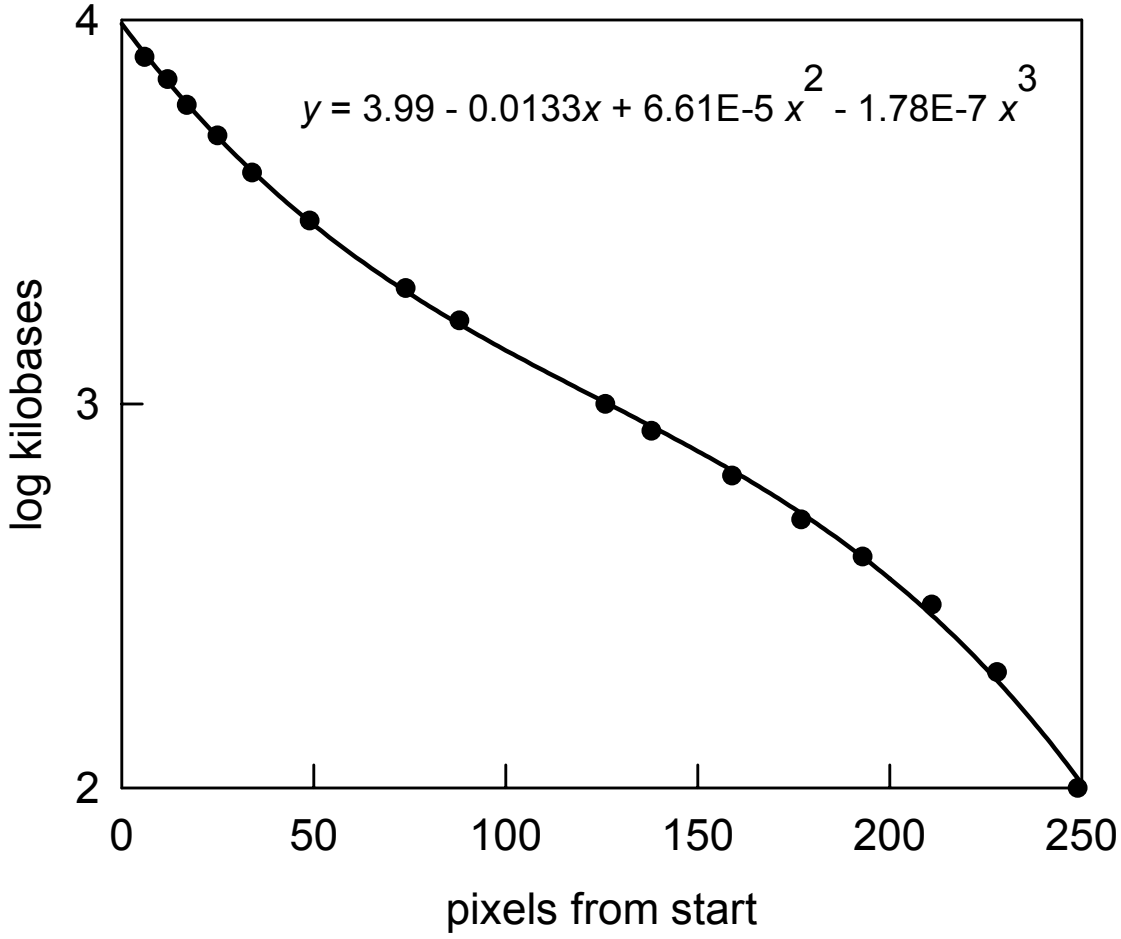

Figure 7. DNA size calibration plot of Figure 6, lane 7 using bands ranging from 100 to 8000 base pairs. This data predicts sizes of 3390 (± 70) bp for the fragment in lane 5 (known to be 3500 bp) and 3120 (± 60) bp for the "unknown" fragment in lane 9. The predictions include correction for a small linear drift in the *x* position of a given band with increasing lane number, and the uncertainties are assigned by assuming that the peak pixel position of a band could be off by ± 1 .

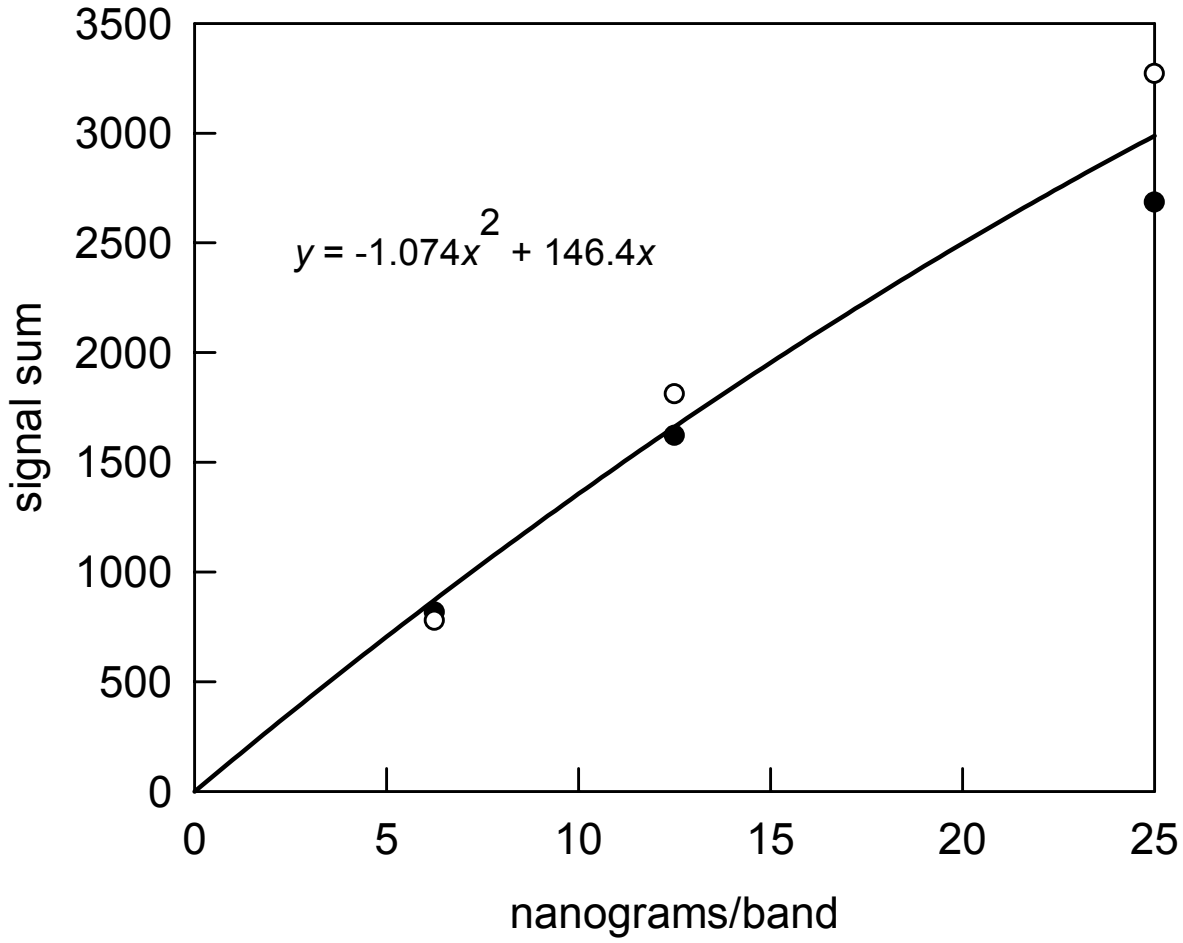

Figure 8. Signal intensities vs. concentration for the 3000 (solid points) and 4000 (open points) bp peaks in the DNA ladder standards. This standard curve allows reasonable estimates to be made for the amounts of samples of similar size.

Figure 9 shows a processed image of a protein electrophoresis gel[2], along with a LabVIEW deconstruction of several overlapping bands in the densitometry plot of a yeast sample in the third lane from the top. A Levenberg-Marquardt non-linear fitting algorithm finds the ten best-fit Gaussian bands for this data. The ability to select certain regions for more detailed study can be very useful in comparing the relative amounts of various fragments from different samples, and in detecting the presence of new fragments in modified samples.

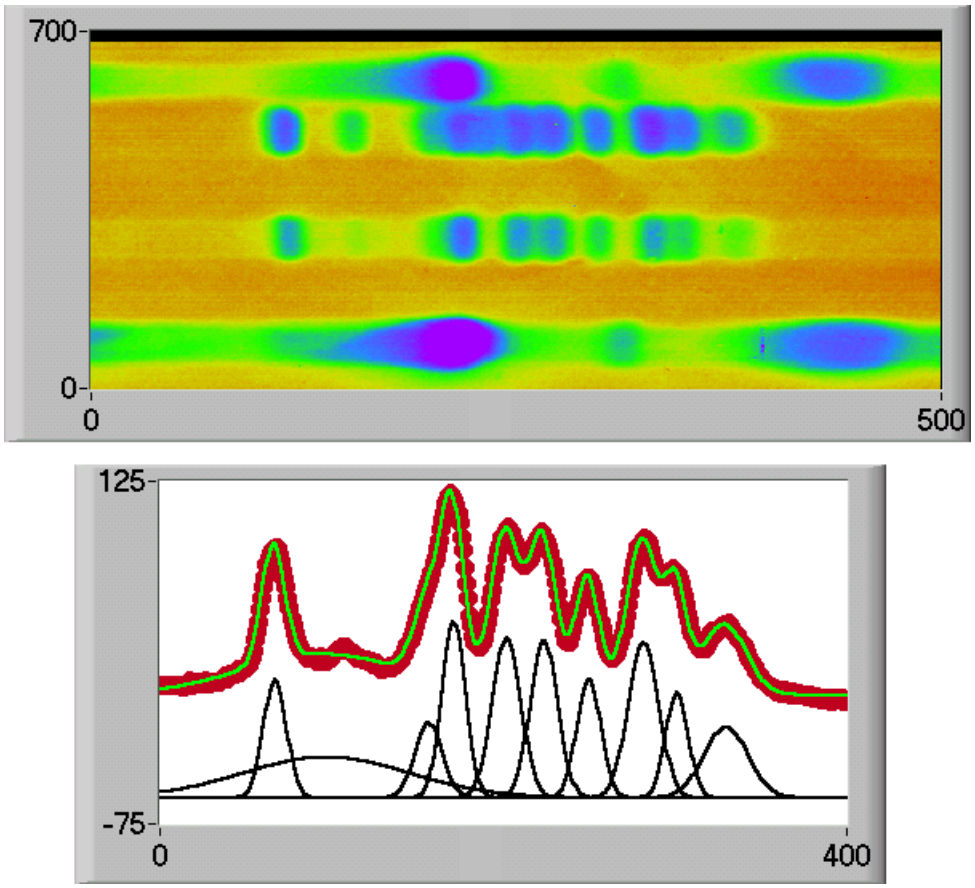

Figure 9. The upper LabVIEW panel for this protein electrophoresis gel image displays intensity plots for two related strains of yeast protein (lanes 2 and 3 from top), in addition to standards. In this example, a *y*-sum plot for lane 3 is shown as the thicker points line in the lower graph. The thinner line overlapping the data shows the fit results using ten Gaussian bands, and the individual best-fit components are also shown as offsets.

Example 4: Kinetics of toluidine blue reduction by sulfite *(6).*

$$TB^{+}\ (2 \times 10^{-5}\ M,\ blue,\ \lambda_{max} = 633nm) + SO_3^{2-}\ (0.180\ M) + H_2O \rightarrow TBH\ (colorless) + SO_4^{2-} + H^{+}$$

The previous examples deal with single static images and most of the discussion has focused on the software analysis rather than the image acquisition. The system also has obvious possibilities for recording color changes in many kinetic systems, including cases such as oscillating reactions *(7)* where color change may be a function of position. In the present example, the focus is on using the camera and image acquisition board to obtain images at programmable time intervals. Figure 10 shows an image of reaction and blank solutions in two adjacent beakers on top of the light box source of Figure 1. This image is obtained by a LabVIEW program which controls image acquisition rate, selects a particular region of interest within the full image[3], compares and stores light levels for comparable areas in the two 30 mL beakers, and then discards the images to avoid excessive use of memory. Toluidine blue in water absorbs broadly in the red, with a maximum absorption at 633 nm and a shoulder near 600 nm. Light from the light box was passed through a red filter, and measurements were recorded by the system at 3 second intervals for the plot shown. The pseudo first-order rate constant of $3.9 \times 10^{-3}\ s^{-1}$ from the plot of Figure 10 (at 18 C) is the same as the pseudo-first order rate reported for a 0.100 M sulfite concentration at 25 ^{o}C *(6)*.

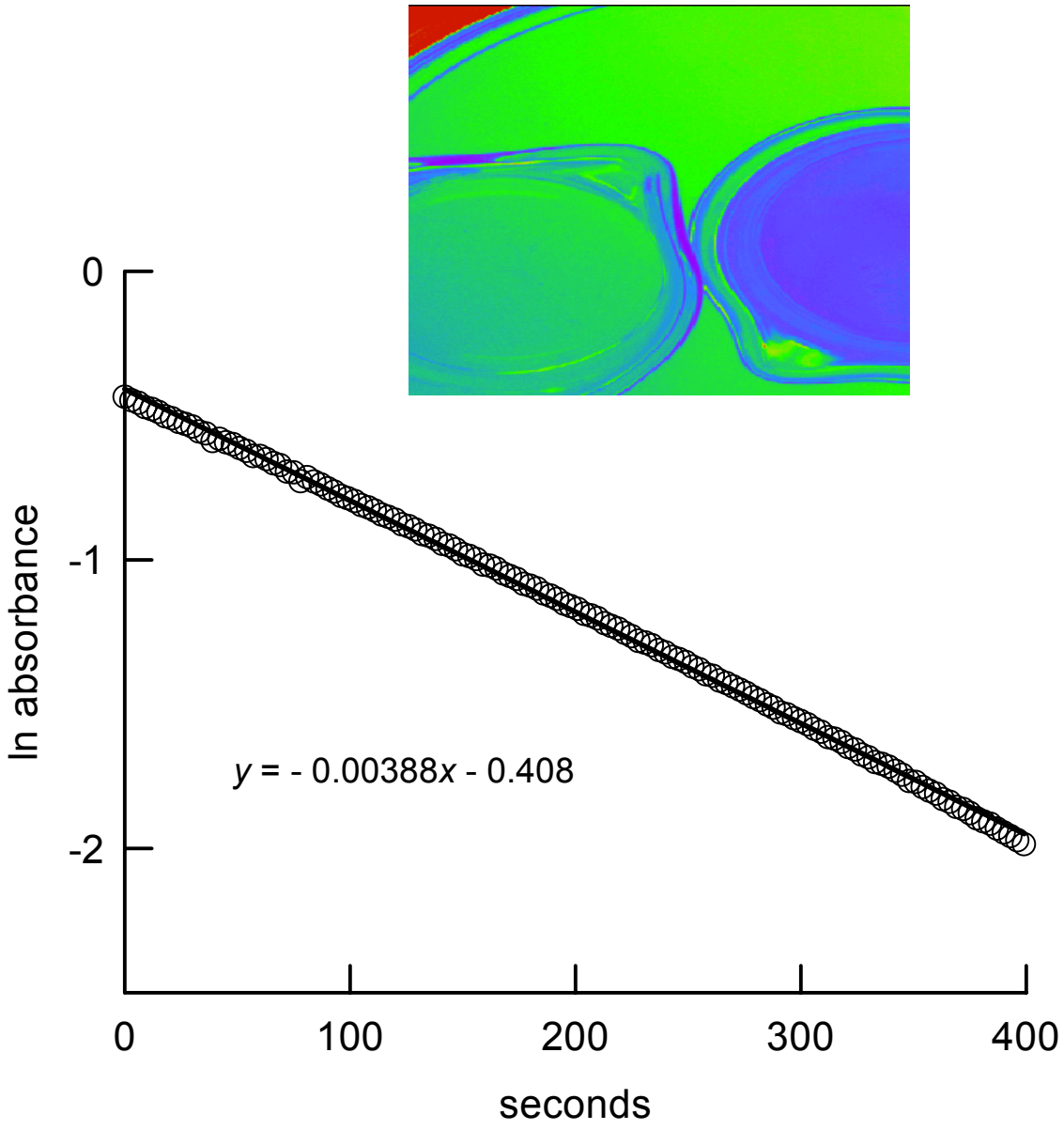

Figure 10. LabVIEW panel and first-order plot for the toluidine blue reduction reaction with sulfite. The right 30 mL beaker contains 10 mL of 0.180 M sulfite, 2 x 10^{-5} M toluidine blue, and the left 30 mL beaker contains 10 mL of the sulfite solution (blank). Solution depth is about 1 cm, and the beakers sit on top of a petri dish filled with a red solution which blocks transmission below 580 nm. Transmittance data is transferred to a spreadsheet for more detailed analysis.

Example 5: Capturing published data

In laboratory studies or advanced course work drawing on the research literature in chemistry, it is often desirable to retrieve quantitative information from published images such as graphs or photographic plates of spectra. Reference *(8)* provides one example of the tools which can be used for such purposes. This can also be accomplished with the present system, as illustrated by Figures 11 and 12. Figure 11 is an image of a published oscilloscope trace *(9)* for HCO UV absorption in the reaction:

$$HCO + HCO \rightarrow \text{products}$$

Figure 12 is a gray-scale intensity plot for the oscilloscope trace, and a second plot which uses the intensity contrast of the image to filter out the coordinates of points on the image of the trace. As discussed further in the *JCE Online* supplemental material, these points can be stored and used to check the second-order kinetics reported for this reaction. After about 50 μs, the slope of the second-order plot from the extracted data, 1.23 μs^{-1} , compares very well with the reported value. A filtering window can also be set to retrieve points from the oscilloscope grid image, enabling the accurate conversion of pixel points to time and transmission values.

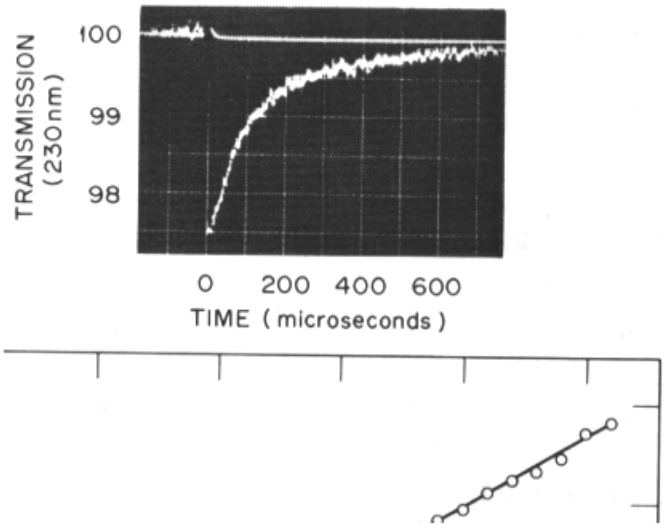

Figure 11. Image of the upper portion of page 233 of reference *(9)*. Data points and grid reference lines on the oscilloscope trace can be extracted by pixel intensity selection software. The upper oscilloscope trace is a "blank" signal.

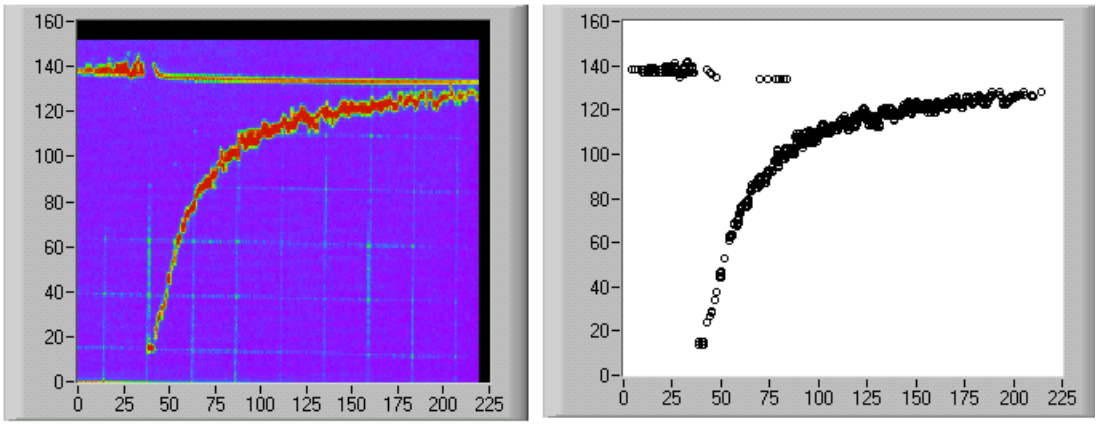

Figure 12. The original version of this LabVIEW panel uses a color ramp to show pixel signal variations in the selected oscilloscope image (left graph). Pixels along the absorption signal trace, white in Figure 11, all have intensity values in the 245-256 range (camera saturation value = 256). These points are selected as a sub-array and displayed in graph on the right. They are also stored in spreadsheet format for further analysis.

Acquisition and Processing considerations

The camera images use an 8-bit intensity scale, and this implied dynamic range of 256 can be extended somewhat by taking images of the same pattern under differing f-stop conditions. Well plate results for systems similar to Example 1 can be meaningful over a concentration range of about 1000. The glass camera lens essentially limits measurements to the visible region. Illumination factors to be considered are the wavelength and spatial intensity distributions of UV or light box sources, the possible influence of spectral spikes in the visible fluorescent lamps often used in a light box, and possible needs for wavelength filtering.

For examples 1, 2 and 4, concentrations of analyte are related to the absorbances of either UV fluorescence excitation wavelengths, or the visible wavelengths transmitted through a sample from the light box. Dark signals are zero for the fairly low camera sensitivies of our examples. "Blank" or "background" signals needed to determine sample transmission and absorbance are easily obtained for the rather uniform light box illumination. The background TLC plate fluorescence for example 2 is found by a quadratic best-fit to two regions of background points selected by the user.[4] For example 3, the measured visible fluorescence induced by the uniform UV illumination is directly correlated with DNA concentration, and conversion to a corresponding UV absorbance is unnecessary.

Parts of the data processing can be accomplished at the IMAQ, LabVIEW or spreadsheet level in the examples of this paper. The *JCE Online* supplemental material for this paper has further information on the examples, including the background planar fitting procedure, the peak deconvolution procedure of example 3, and false-color intensity plots of several of the LabVIEW panels shown above. LabVIEW code for the examples is available upon request.

Acknowledgements

This work was partially supported by a Howard Hughes Medical Institute grant, and by a National Instruments Academic Partner grant. We thank Pam Connerly and Mark Hochstrasser of the University of Chicago for permission to use the yeast protein example shown in Figure 9. We also thank Darren Halla at National Instruments, and Earlham colleagues Mike Deibel, Corinne Deibel and Mark Stocksdale for extensive comments and help with examples 1 – 4.

Literature Cited

1. Johnson, G.W. *LabVIEW graphical programming: practical applications in instrumentation and control*, 1994, McGraw-Hill.
G Programming Reference Manual, 1998, National Instruments Corp.

2. *IMAQ Vision Builder Tutorial*, 2000, National Instruments Corp.
IMAQ Vision for LabVIEW User Manual, 2000, National Instruments Corp.

3. Harris, D. C. *Quantitative Chemical Analysis*, 4th Ed. 1995, W.H. Freeman, 544-545.

4. Switzer, R.L.; Garrity, L.F. *Experimental Biochemistry*, 1999, Freeman, New York

5. Peller, J.R. *Exploring Chemistry: Laboratory Experiments in General, Organic and Biological Chemistry*, Prentice Hall, 1998; p. 265.

6. Jonnalagadda, S.B.; Gollapalli, N.R., *J. Chem. Educ*., **2000**, *77*, 506-509.

7. Scott, S.S.; Schreiner, R.; Sharpe, L.R.; Shakhashiri, B.Z.; Dirreen, G.E. in *Chemical Demonstrations*, Vol. 2, Shakhashiri, B.Z. ed, 1985, University of Wisconsin Press, Madison, WI, Ch. 7 Oscillating reactions.

8. Aymard, C.; Shirts, R.B. *J. Chem. Educ*., **2000**, *77*, 1230-1232.

9. Hochanadel, C.J.;.Sworski, T.J.; Ogren, P.J. *J. Phys. Chem*. **1980**, *84*, 231-235.

Footnotes

1. The background fluorescence level can be described by a slightly curved intensity surface over the plate area. UV absorption by sample molecules reduces the fluorescence signal, and we expect an experimental absorbance defined by $A_{xy} = \log(signal_{xy} / background_{xy})$ to be correlated with UV absorption and with moles of sample at each *xy* pixel.

2. This example uses the IMAQ/LabVIEW software to process a TIFF image obtained elsewhere, using a scanner to obtain a digital image of the original gel. The relationship between concentrations and intensity values is difficult to estimate here because the acquisition hardware parameters are not known. The simple use of pixel intensity values is probably reasonable for the comparison of similar samples.

3. IMAQ software automatically creates LabVIEW code for the operations invoked by the user. Thus, we use the IMAQ system to acquire a single image similar to Figure 10 and select a region of interest (ROI). The image acquisition/ROI script created during these operations is then modified slightly and inserted into the loop structure of the LabVIEW kinetics code so that images may be acquired and processed at set intervals.

4. Typical standard deviations of the fit are 2 – 6 units (1 – 3% of the maximum signal range of 256). In some cases, the distribution of residuals is clearly not random, indicating some inadequacies in describing the surface with a quadratic model.

Supplemental Material (for *Journal of Chemical Education Online*)
This material includes further information on system components, and on the five examples discussed in the main paper. The literature citations and figures in this section are continuations of those in the main paper, with additions numbered in sequence.

Acquisition hardware and software
A. Hardware:
Computer system: Gateway 800 MHz system running Windows 98
National Instruments PCI 1407 video board $895, less educational institution discount
Camera: Graftek, Inc. SONY XC-73 monochrome machine vision camera. $725
The images are captured and recorded in a 640 x 480 pixel format, with a dynamic intensity range of 8 bits per pixel. Specifications for the camera show a linear relationship between light levels and CCD signals up to saturation, with little variation in pixel sensitivities. Complete camera specifications are available at
http://www.sony.co.jp/BizPartners/ISP/
V2513 25 mm lens $128 or HS 16A-2MI 16 mm lens $198. The latter captures a wider field angle for higher pixel resolution of important image subfeatures.
Light box, homemade camera stand, optical filter sheets or solutions.

B. Software systems
LabVIEW 6i, version 6.0.1
IMAQ Vision Builder 6.0
IMAQ Vision for LabVIEW, version 6.0.1
NI-IMAQ 2.5 version of the video board driver (free download with board)

Comparative costs: The total hardware cost for the system with a 25 mm lens is about $1750. The LabVIEW Full Development System package needed to write or modify programs is $1900 for educational institutions. This includes a 10-station license, renewable and upgradable at an annual fee of $400. The IMAQ software may also be obtained with a 10-station license (total of $1495, renewable and upgradable for an annual fee of $395.) These costs may be compared, for example, with commercial densitometry units ranging from list prices of $2900 for a basic unit (Bio-Rad Wide/Long Documentation System: UV illuminator, Polaroid camera, no software) to $10,000 (Bio-Rad Gel Doc 2000 Gel Documentation System: UV illuminator, CCD camera, software).

Software used for the examples: Four LabVIEW programs have been written for the examples of the paper: All are available upon request.
1. IMAQ_SAT used for examples 1, 2 and the first part of 3. This opens TIFF images, allows the user to select two background regions for fitting to a background signal surface, and then processes selected portions of an image in one of three selectable modes: S (signal – background), A (absorbance) and T (transmittance). The data typified by the final plots for examples 1 and 2 can be stored in spreadsheet mode for further analysis.
2. IMAQ_GAUSS used in processing the data of Figure 9.
3. IMAQ_KIN used in the kinetics example.
4. IMAQ_READER used in example 5 for data extraction from published material.

Example 1 details.
A stock solution of 2×10^{-4} M toluidine blue O (Aldrich) was prepared for this example and for Example 4. An Eppendorf pipet was used to prepare the dilutions and fill each well with a standard volume of solution (0.250 mL). Figure 1 is repeated here in color mode.

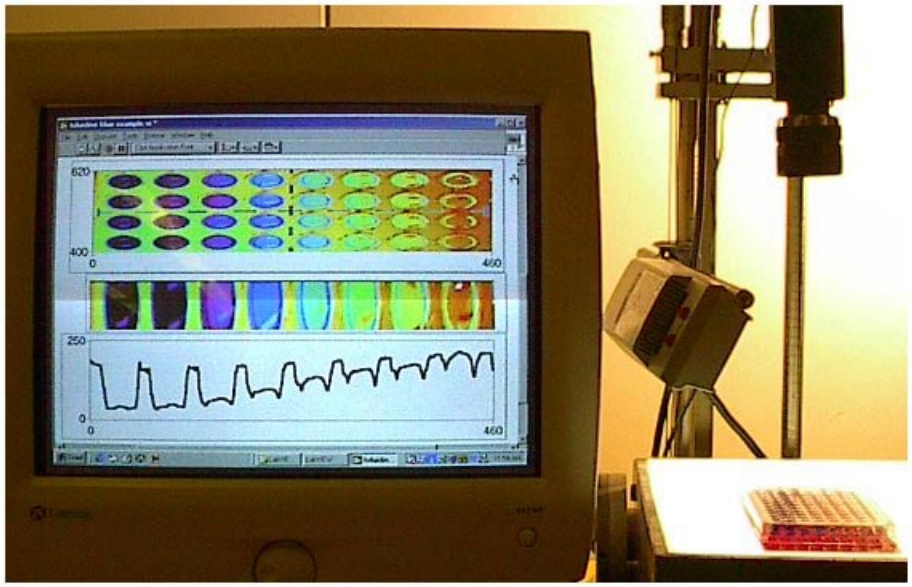

Figure 1 in color

The intensity scale ranges from near zero = black/dark purple to 250 (red) in the computer image. There is some variation in the light intensity field of the light box as can be seen by the shift in background colors between the wells, and this can be easily corrected by fitting the background intensity surface. However, for introductory purposes, we have chosen to display the raw pixel values with no background correction. The data of the lower graph were then processed in Excel to obtain Figure 2. For example, the low signal value in the middle of the first well on the left is proportional to light transmission, and the average of the high values on either side of this well gives a "blank" transmission for light coming through the plastic material of the well plate. The "blank" well signal, on the right of the graph, is essentially the same in the middle as the two adjacent high values, demonstrating that use of "blank" values from the "plastic only" regions is a reasonable strategy for processing the data.

Example 2 details.
A standard solution of 50 mg acetaminophen and 50 mg of acetylsalicylic acid was prepared in 20 mL of 50:50 ethanol:methylene chloride. Aspirin and Tylenol tablets, each stated to contain 325 mg of active ingredient, were dissolved separately in 100 mL of 50:50 ethanol:methylene chloride. Some tablet binder remains undissolved in each case. TLC plates were prepared by using one or more applications of standard or sample from a capillary spotter to the plate starting line. The plate was then eluted in 50:50 hexane:ethyl acetate containing 3% glacial acetic acid. The fluorescent TLC plates were Whatman PE Sil G/UV. We have found no significant difference between standard curves obtained by multiple applications using the same capillary and same concentration of analyte, and curves obtained from single applications of different concentrations. Multiple applications are clearly simpler in practice. We have tested both our own capillaries, obtained by pulling glass in a flame, and commercial 5 μL microcapillary pipets (Aldrich). Our capillaries give smaller spots, a desirable quality. (Our estimated volume per application is 1 – 2 μL). However, our capillaries also give larger variability in the transferred volume unless they are prepared carefully. A key factor is producing a clean flat tip, and one practical way to get this is to lightly scratch the capillary across the slightly rough top edge of a Buchner funnel before breaking it to produce the final applicator. Our typical standard deviation in volume transferred by single applications to the TLC plate is about 13%, and multiple applications of N transfers should reduce sample size uncertainty by $1/\sqrt{N}$.

Figure 13 shows the full computer panel display of the LabVIEW program IMAQ_SAT which we have used to analyze the image of the acetaminophen/aspirin example in the absorbance mode. The upper display shows the image of the TLC plate, acetaminophen spots near $x = 250$ and acetylsalicylic acid spots near $x = 50$. The solvent front is near $x = 20$, and the starting line would be near $x = 325$. The starting line was not selected in the IMAQ acquisition step because the focus of this example is on spot intensity analysis rather than R_f values. The two expansion regions in the next two intensity displays show the regions used for determining the background surface. The BACKGROUND PLANE CORRECTED display is in absorbance units. The image is rotated 90° and the final analysis region is then selected for the display plot. The latter trace is obtained by adding the absorbance values along the entire y range (250 - 300 in this case) for each x value. This plot trace was transferred to Excel and areas under each of the four standard peaks were used to determine the total absorbance values used in Figure 5. For this example, the standard solution is equivalent to 250 mg acetaminophen/100 mL solvent. Three capillary applications of the Tylenol solution were made to produce the sample spot. (1 tablet broken up and maximally dissolved in 100 mL solvent).

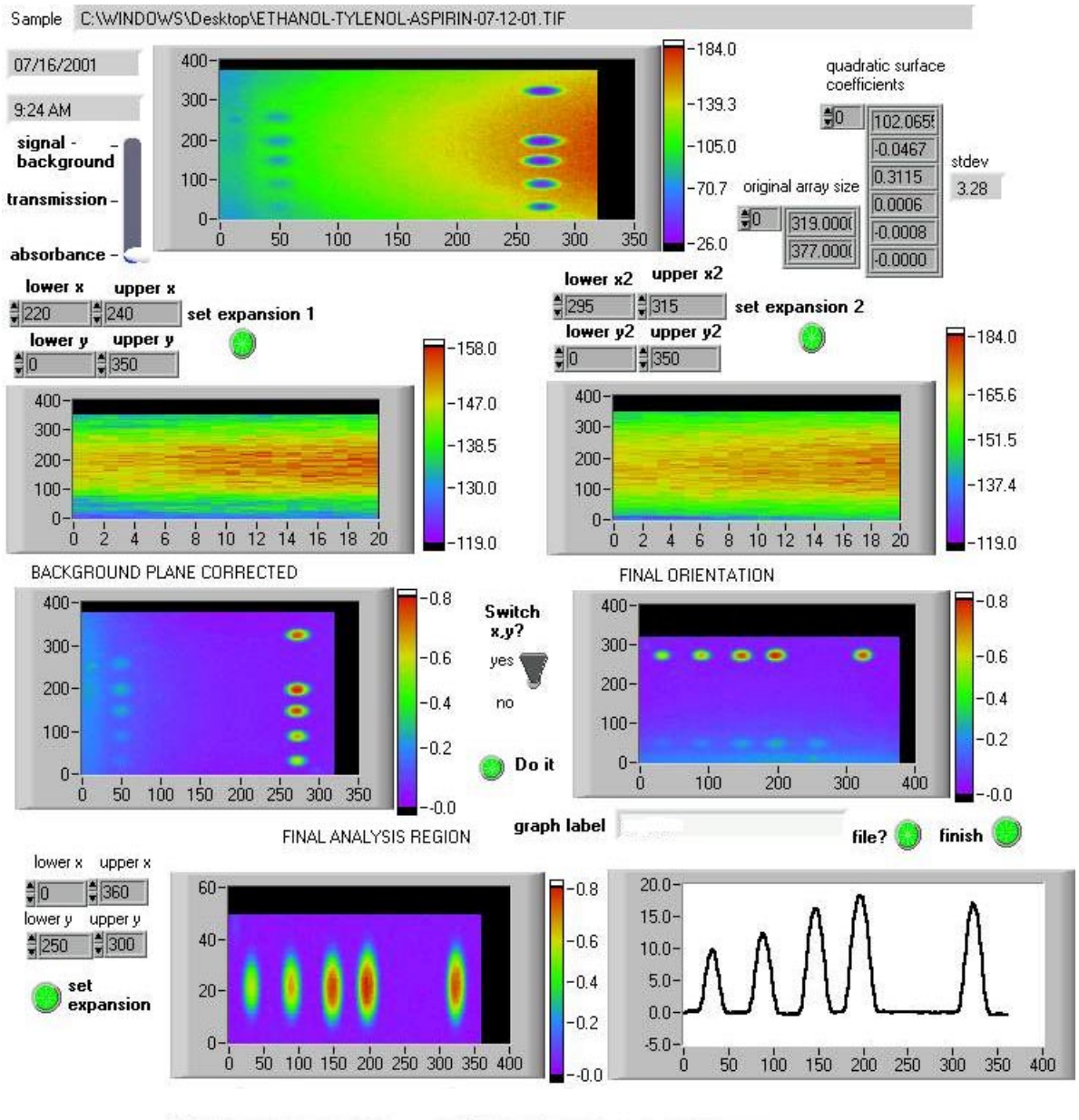

Figure 13

The absorbance sum for the Tylenol sample was 329, and the calibration curve implies that this total would correspond to 4.02 transfers of the standard. The amount of Tylenol in the solution prepared from one tablet is then: $x = \frac{4.02(250 \text{ mg}/100 \text{ mL})}{3} = 335$ mg/100 mL , or 335 mg in the tablet. The uncertainty is estimated from $13\%/\sqrt{3}$ using the information cited above on application volume variability.

A similar treatment was used to evaluate the aspirin spots, with the results shown in Figures 14 and 15. In this case, the lowest aspirin concentration is difficult to detect, and the signals for several of the spots are small enough for deviations in the baseline from the zero correction to be significant. Nonetheless, it is clearly possible to extract reasonable information for a calibration graph.

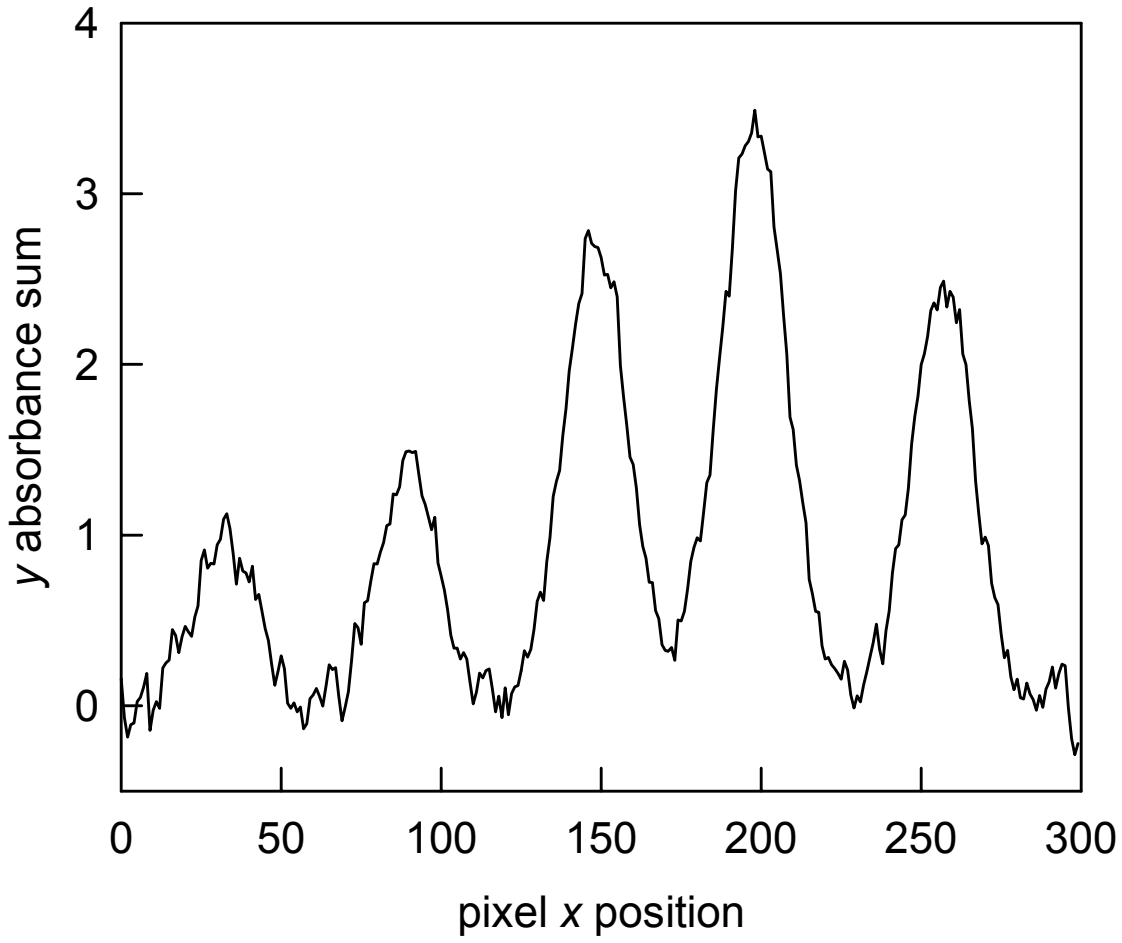

Figure 14. The *y* sum plot for the aspirin spots of Figure 13. The first four peaks are spots from 1, 2, 3 and 4 applications of the acetylsalicylic acid standard, and the right peak is from an aspirin tablet.

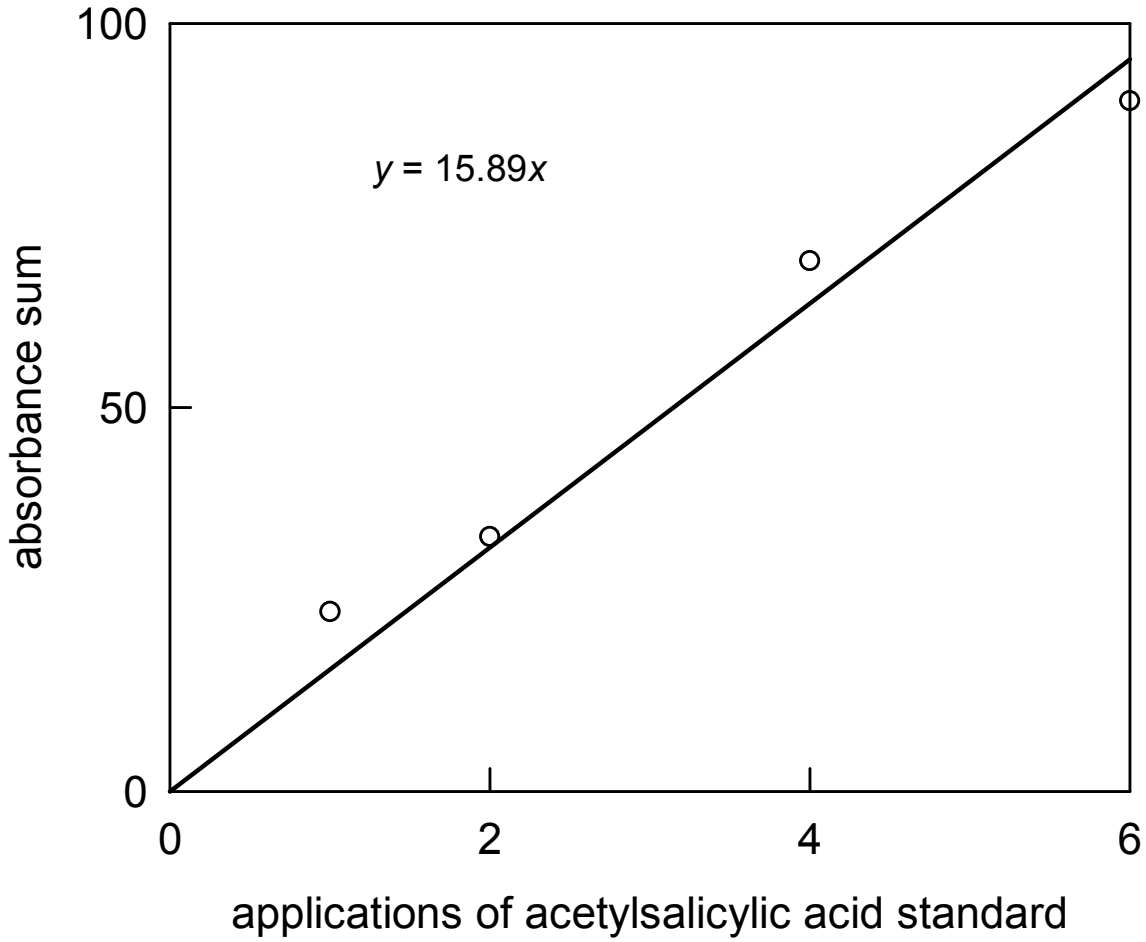

Figure 15. Aspirin calibration: Total intensity vs. applications of acetylsalicylic acid (50 mg/20 mL 50:50 ethanol:methylene chloride solvent). The aspirin sample of Figure 14 (1 tablet extracted with 100 mL of 50:50 ethanol:methylene chloride, 3 applications to the TLC plate) gives an absorbance sum of 60.6, corresponding to 3.81 applications of the standard. This converts to 318 (± 8%) mg for the aspirin tablet, vs. 325 mg stated by the manufacturer.

The TLC spots of this example are detected by fluorescence suppression. In a well-focused image, we make the assumptions that each pixel records intensity from a well-defined geometric region of the image, that image regions covered by one pixel are not covered by other pixels, and that the image region is fully covered by the pixel field. Under these circumstances, a simple model for the signal S_{xy} at each (x,y) pixel is that it will be proportional to the UV light reaching the corresponding image region on the TLC plate surface. We let S_{xy} represent the fluorescence signal from a region with absorbed analyte, and then compare this with $S_{xy,o}$, the signal expected for no analyte. The difference is primarily due to UV absorption by the analyte, so one might expect that the usual form of Beer's Law would give information about sample amounts in each imaged region:

$$A_{xy} = \varepsilon n_{sample,xy} = -\log\left(\frac{S_{xy}}{S_{xy,o}}\right) \qquad (1)$$

where A_{xy} is the absorbance measured at an image position corresponding to pixel x,y and ε is the extinction coefficient for the UV light. Here, $n_{sample,xy}$ is the moles of sample absorbed on the plate surface imaged by particular pixel; this replaces the usual Beer's Law cl terms because the sample is not in solution.

The absorbance sum numbers for each spot used in Figures 5 and 15 are given by the double sum:

$$A = \sum_x \sum_y A_{xy} = \varepsilon n_{spot} \qquad (2)$$

If the simple model were completely accurate, one would expect that a plot of A vs. sample size would be linear, with a zero intercept as is generally true for monochromatic light sources in solutions or gases. In fact, however, the standard curve of Figure 5 is non-linear. Factors which may contribute to this include: a) differences between the behavior of surface absorption sites and deeper sites in the thin layer; b) fluorescence contributions from the analyte molecules; and 3) the fact that the excitation source, a Hg lamp, has multiple UV wavelengths. Generally we have found linear calibration curves with intercepts close to zero for low absorbance values (maximum pixel absorbances of 0.7 or less), and non-linear curves for more intense spots.

There is a tradeoff between the desirability of a linear calibration and signal-to-noise problems at low spot intensities. The clear evidence for a non-linear curve in Figure 5 raises an important issue for the analysis because it suggests that equation (1) might work well for pixels imaging regions of low analyte levels, but poorly for pixels imaging regions with high analyte levels. In that case, the sum of equation (2) would of course no longer be proportional to the total amount of analyte, and furthermore, this sum might depend upon how much the analyte spot was spread out over the TLC plate. These difficulties strongly imply that the standard and sample chromatography conditions must be very similar. Since that is to be expected in this example, the use of a non-linear calibration curve, with standard points bracketing the sample point, is still a reasonable approach for extracting quantitative information on the sample.

The experimental conditions for good measurements include a sufficiently strong fluorescence signal from the TLC plate and a camera f-stop setting which does not saturate any of the CCD pixels. It is clearly desirable to have a fluorescence signal which is both uniform and strong, but this is difficult to achieve with the hand-held UV source of Figure 1. It is possible, however, to have a fluorescence background field with a tilted and slightly curved intensity profile. This can be adjusted and set interactively using IMAQ-level features which provide 3D projection plots. The UV source is clamped in a more permanent orientation once optimum fluorescence background conditions have been achieved.

It would be possible to correct for much of the fluorescence background variations over the camera field of view by subtracting a "blank" signal from a clean TLC plate. However, equation (1) implies that it is important to know an accurate background signal $S_{xy,o}$ at each pixel. Therefore, instead of background subtraction, we use background regions in the experimental TLC plates to fit the background signal surface with a quadratic surface described by:

$$z(x, y) = a + bx + cy + dx^2 + ey^2 + fxy \qquad (3)$$

This is a standard problem in multiple linear regression *(10, 11)*. LabVIEW provides routines for polynomial functions of x, but does not appear to have corresponding routines for two independent variables x and y. However, the six-parameter set $\{a..f\}$ can be evaluated in one cycle of computations involving construction and inversion of a 6 x 6 curvature matrix. For example, if the fit is over a 50 x 70 region of pixels, for each pixel i there will be a set of 6 terms $\left\{1, x_i, y_i, x_i^2, y_i^2, x_i y_i\right\}$ with 1 being the coefficient of a in equation (3). Sums of products of these terms over the 3500 pixels in this region, such as $\sum_1^{3500}\left(x_i^2\right)\left(x_i y_i\right)$, constitute the 36 elements of a symmetric 6 x 6 curvature matrix. Sums of products of these six terms with $z(x_i,y_j)$ also give a six-term "z vector" which can be used with the curvature matrix to compute a best-fit solution vector $\{a,b,c,d,e,f\}$. The standard deviation of typical fits is 2 – 6, and is in reasonable agreement with pixel-to-pixel response variations to a constant light level. In some cases there is non-randomness evident in the distribution of deviations from the fit, indicating that equation (3), while simple, may not be the optimum choice for the fitted surface.

Once the $z(x,y)$ surface is obtained, LabVIEW computation of the A_{xy} values via (1) is straightforward. The time required for the fitting and absorbance sum computations for a 300 x 300 surface is less than 1 second in our system.

Example 3 details.
This example is part of a study seeking to amplify a particular gene using PCR in an undergraduate research project conducted by Mike Deibel and Mohannad Kafri at Earlham. An E-Gel 1.2% agarose system (Invitrogen) was used. The DNA electrophoresis ladder was a 20 fragment 1 Kb Plus standard (Gibco), stock concentration 0.1 μg/μL . 20 μL volumes of standards and samples were added to each lane. The ladder patterns in lanes 3, 7 and 11 are for dilutions of the ladder stock by factors of 1/4, 1/8, and 1/16 . A PCR control band at 3500 bp appears in lane 5, and the target gene is in lane 9. The UV illumination source is a Fisher Biotech FBTIV816 system operating at 312 nm, and the orange fluorescence from ethidium bromide bound to the DNA is passed through a Kodak Wratten 22 (Sigma) filter in front of the camera lens. The primary goals in an experiment such as this are to identify the number and size of the target fragments, and to obtain a reasonable estimate for the amount of the target genes prepared.

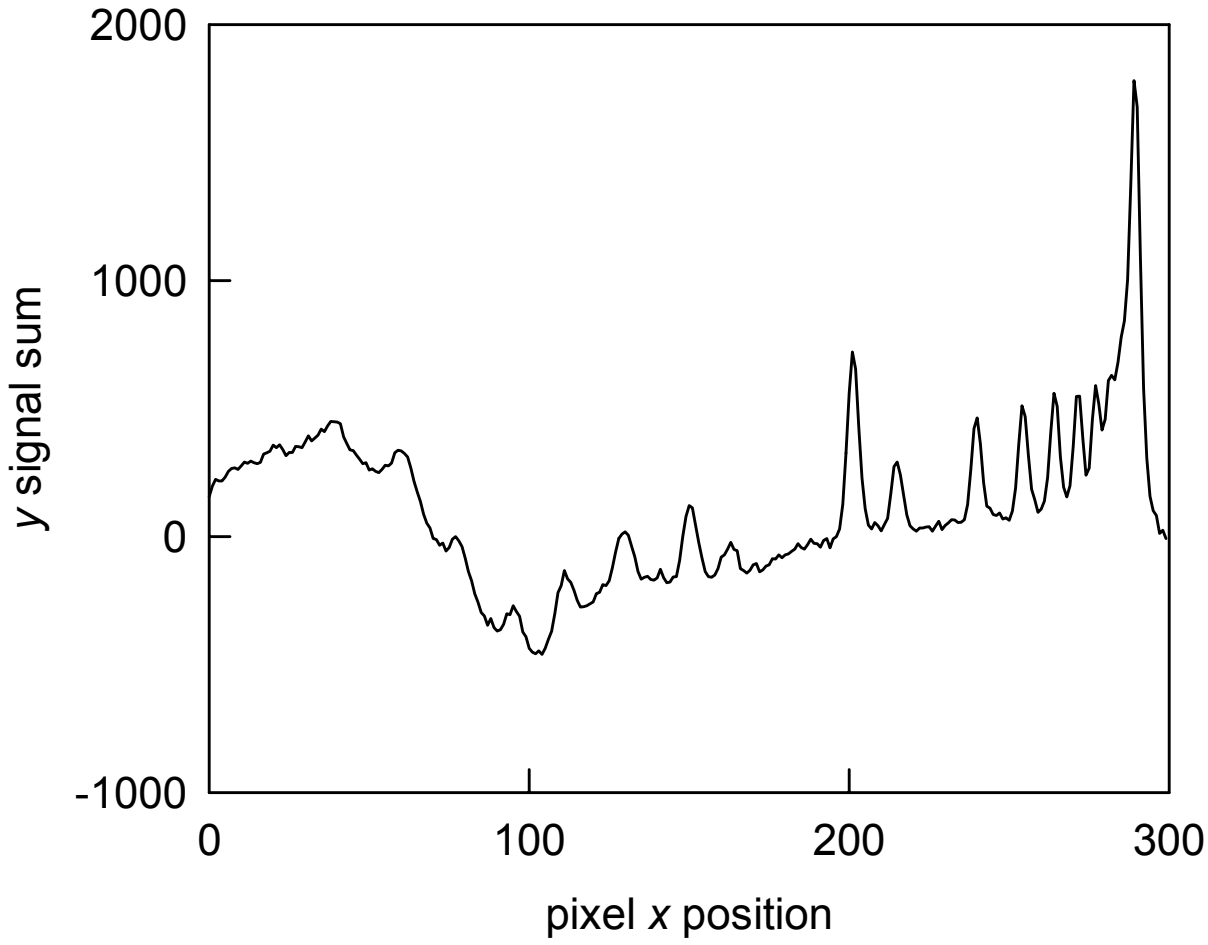

Figure 16 Densitometry plot for lane 7 of Figure 6. The *x*-axis represents pixel distances in the vertical direction of Figure 6, and the origin of the electrophoresis is at pixel 289. Signal – background is evaluated at each pixel, and the *y*-axis plots the sums across the bands of lane 7 for each *x* position along the lane.

Data for the construction of Figures 7 and 8 was acquired with the IMAQ_SAT program in the signal – background mode. A plot of the results for the lane 7 data is shown in Figure 16, and the signal peak positions were used with the size assignments from the information supplied by the manufacturer to construct Figure 7. A linear calibration graph is normally used for this type of data *(4, pp. 76, 88)*, which is reasonable over a limited size range. We have used a cubic polynomial (Excel trendline option) which more accurately describes the curvature of the plot over a larger fragment size range. The curvature on the left end is easily understood because one would expect the plot to approach the *y*-axis asymptotically.

We expect the visible fluorescence from the ethidium bromide to be correlated with DNA fragment concentrations, although the correlation will not necessarily be linear. There is considerable background variation, especially in the vicinity of the methylene blue markers, and the background surface was determined by blank regions in the vicinity of the 3000 bp peak for purposes of constructing Figure 8. The points on the plots of Figure 16 are again sums of the band values along the "*y*" coordinate for each "*x*" position. Not surprisingly, this summation always improves the signal-to-noise ratio in comparison with plots of data along the centers of the bands, and summation along the *y* coordinate also represents the amount of absorbing material more accurately.

The yeast protein example presented in Figure 9 and reproduced in color below is almost in the category of Example 5 in that we have simply analyzed data that was already available in an image file. The protein samples shown in the figure resulted from extensive purification procedures at the University of Chicago, and this provides a very clean image with a nearly flat background in each lane. The analysis displayed in the lower part Figure 9 is similar to the decomposition of overlapping bands in other chromatography problems, and is subject to familiar cautions on the procedure and interpretations. We have assumed Gaussian band shapes in our analysis, and this will introduce systematic errors in the conclusions if the bands are in fact skewed. Each Gaussian band is characterized by three

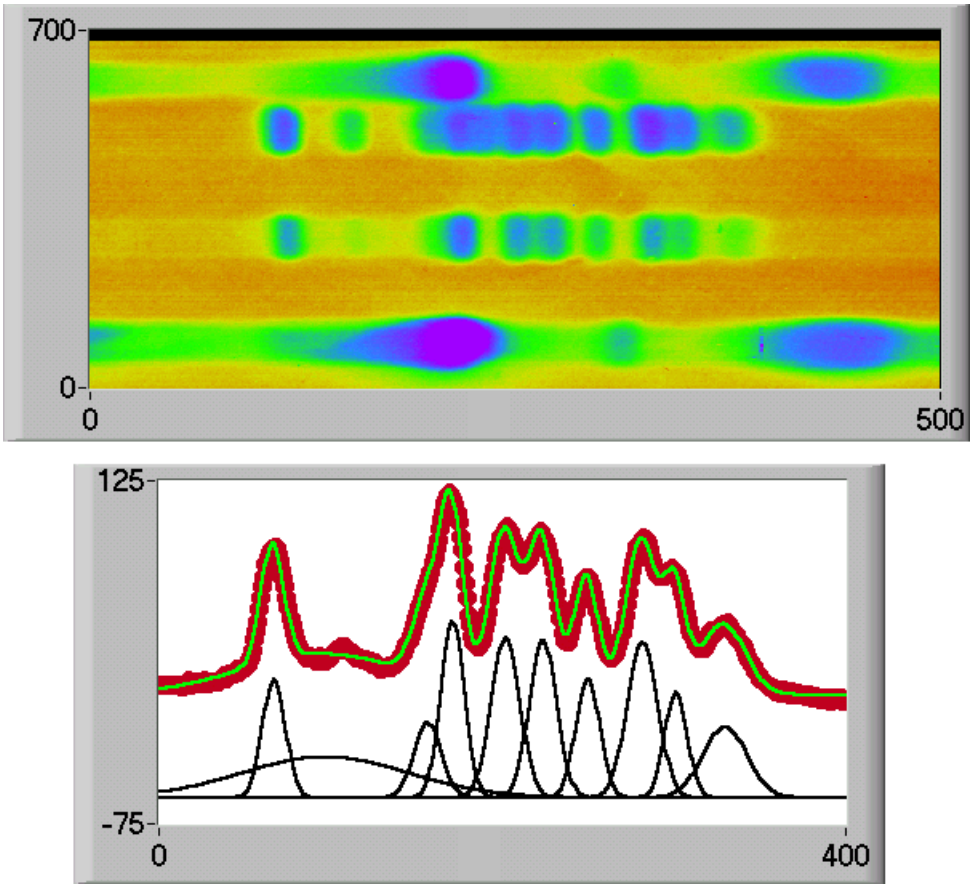

Figure 9 in color

parameters: band center, height and standard deviation. This leads to 30 adjustable parameters for ten bands. The initial baseline and the baseline slope could also be adjustable, but the background correction constructed by the same procedure used in Example 2 allows these values to be fixed at zero. Fixing these values makes it more likely that the iterative fitting procedure will converge to a physically reasonable solution. Even if the solution looks good, however, one must recognize that correlations between peak parameters allow significantly different choices which may give fits of comparable quality. The only way to thoroughly evaluate uncertainties for a problem this complex may be a Monte Carlo procedure *(12)*. Figure 17 and Table 1 show a comparison of relative peaks and areas for lanes 2 and 3 of Figure 9. Lane 2 has one new protein fragment near pixel 180, and the results suggest reasonable estimates for quantitative comparison.

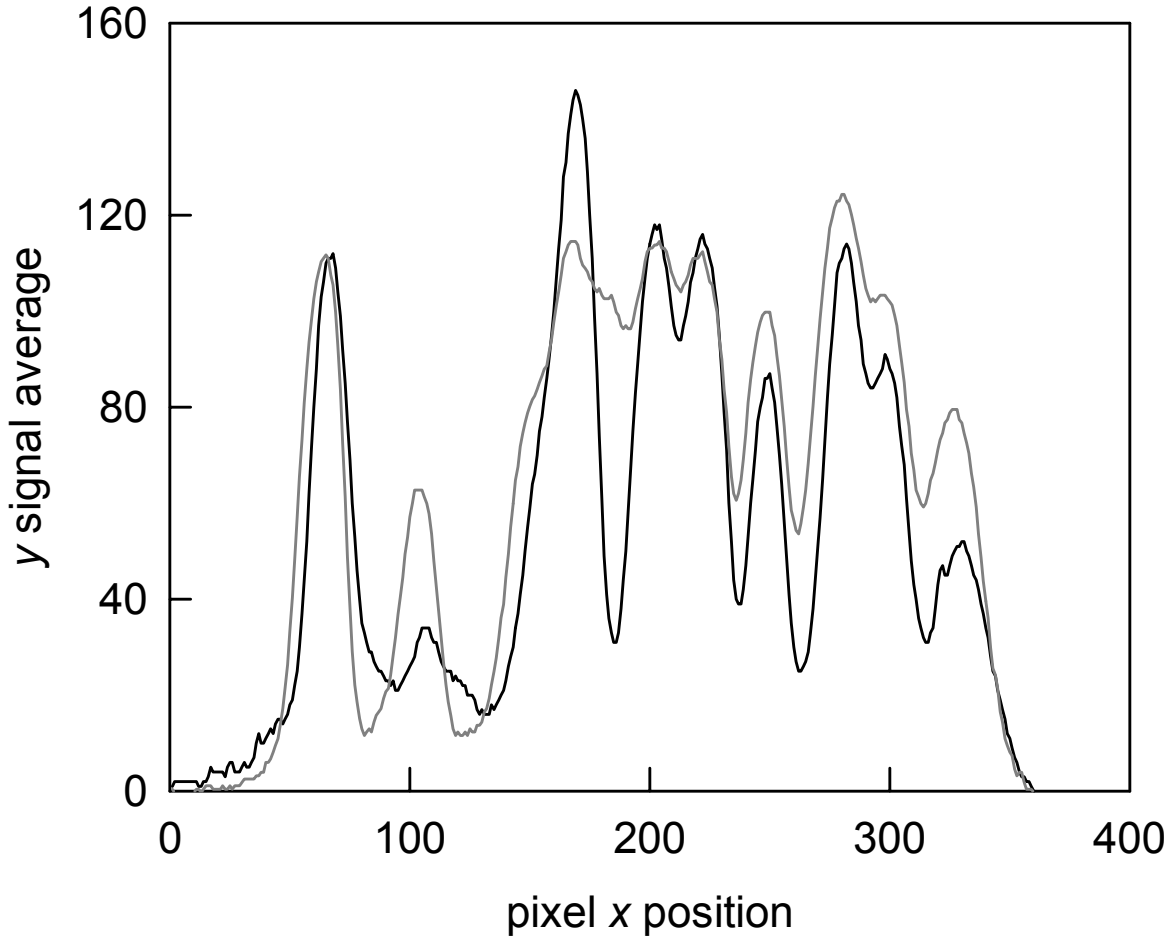

Figure 17. The darker curve is a densitometry plot for lane 3, also analyzed in the lower part of Figure 9. The lighter curve is the corresponding plot for lane 2, for protein isolated from a variant yeast form. Note the indication of a possible additional band for lane 2 near pixel *x* position 180.

Table 1 Fractions of total areas for lanes 2 and 3. Pixel positions refer to Figure 17.

band	1	2	3	4	5	6	7	8	9	10	11
pixel *x* value	65	105	156	170	180	202	224	248	280	301	328
lane 2	0.11	0.06	0.11	0.03	0.07	0.14	0.08	0.08	0.15	0.07	0.10
lane 3	0.11	0.07	0.11	0.09	------	0.13	0.12	0.08	0.13	0.07	0.09

Individual areas are determined from the best-fit Gaussian parameters using 10 Gaussian bands for lane 3 and 11 Gaussian bands for lane 2.

Analyzing images for positional information is obviously not difficult, but the retrieval of valid intensity data may be another matter. One strong caveat for analyzing images for intensity comparisons is that the original images must be obtained under conditions where key pixel signals are not saturated. If software has been used to modify an image, as we have done in Figure 6 to improve the visibility of the DNA bands, then comparative intensity analysis will be worthless. Another common problem is that a few pixels in some systems may be non-functional. This is more likely to be true of "commercial grade" cameras than machine vision cameras. In the image of Figure 9, a few values in the TIFF image were zero, and this leads to problems in using the absorbance mode of the IMAQ_SAT program.

Example 4 details.
30 mL beakers without scratches on the bottom were selected. The beakers were also roughly matched for similar glass distortions on the bottom and for similar diameters. The "blank" beaker of figure 10 was filled with 9 mL of 0.200 M sodium sulfite solution and 1 mL of water. Another 9 mL of sodium sulfite in the sample 30 mL beaker was quickly mixed with 1 mL of stock 2 x 10^{-4} M toluidine blue, (cf. example 1 above) and then the kinetic run was started. Reference *(6)* presents a much more extensive set of results, including a study of ionic strength effects. There were other significant differences with *(6)*. Aldrich reports a certified dye content of 82%, λ_{max} = 626 nm for the toluidine blue O, which we used as received. Using a Perkin Elmer Lambda IV spectrophotometer with 1 nm slit settings, we measure λ_{max} = 633nm for a 2 x 10^{-5} M aqueous solution, ε_{max} = 37,400 $M^{-1}cm^{-1}$. Reference *(6)* reports λ_{max} = 596 nm, ε_{max} = 35,000 $M^{-1}cm^{-1}$ for recrystallized toludine blue, and we note a shoulder in that vicinity for our sample. We have not explored these differences further because our only goal in this example is to suggest the potential for similar kinetic applications of the imaging system. We have not tried to thermostat the system in this example. A simple addition would be to set the beakers in a small water bath with thermostated external coolant circulation lines. It could also be useful to explore replacing the broad band light transmission source with diffused narrow band LED sources *(13)*.

An image is acquired and analyzed at time intervals selected by the user, and the programming requirements for this are straightforward. As noted earlier, IMAQ automatically creates LabVIEW code corresponding to the operations invoked by the user (e.g. acquiring an image, selecting a feature within the image, image rotation, etc.) The results for an image acquisition followed by selection of a Region of Interest (ROI) are shown in the code portrayed in Figure 18.

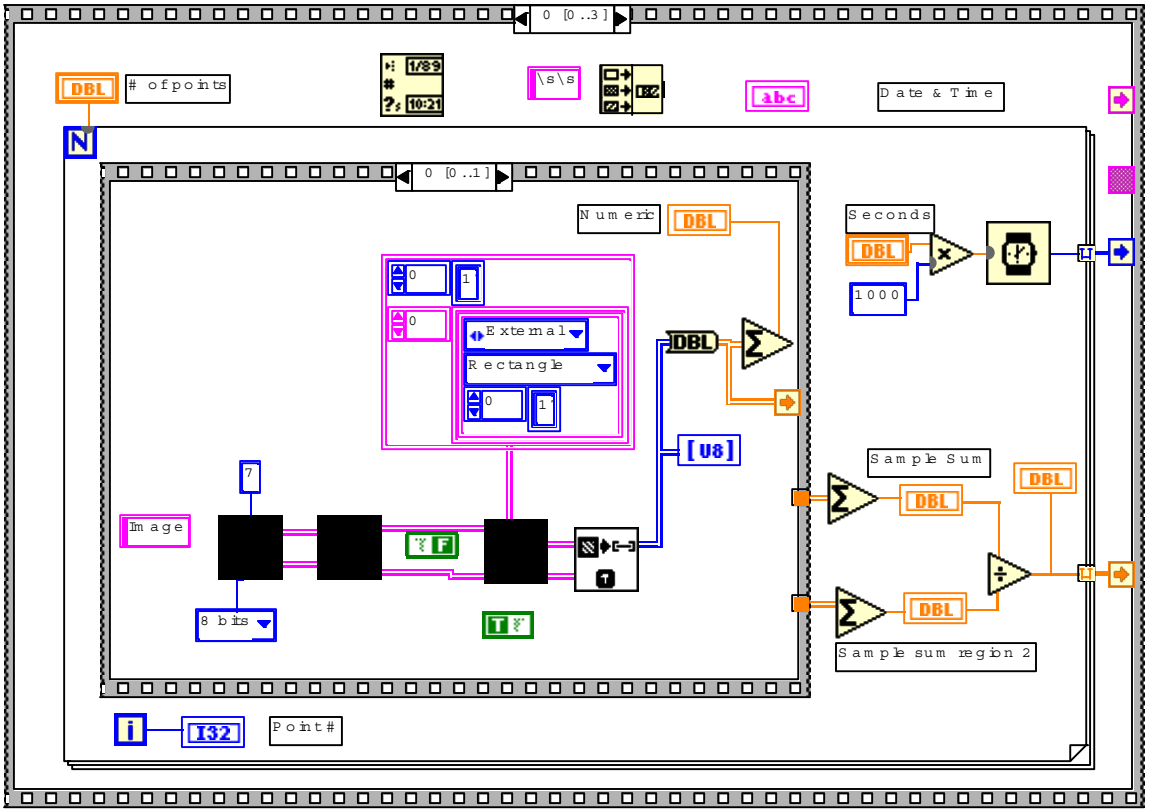

Figure 18. Code created by the IMAQ LabVIEW script builder is shown within the inside " 0 [0..1] " slide frame. The rectangle containing "External", "Rectangle", etc. is a "cluster" used to define a "region of interest" (ROI). The original code was modified by the insertion of the "snap" icon to take a new image. This code acquires an image for each operation of the N-loop, and loop operations are delayed by the "Seconds" input.

At each loop step, the selected portions of the ROI are used to get the light transmission value given by T = *sample signal/reference signal*. The sample and reference signals are actually sums of signals over comparable image regions in the sample and reference beakers, and the code shown in Figure 18 includes computation of the sample signal summation. Since the images are not stored, these features avoid the accumulation of large numbers of TIFF files. All of this processing does require some time, and in our system the maximum repetition rate for Example 4 is about 10 Hz. This is fast enough for many studies, but significantly slower than the 30 Hz maximum frame rate of the camera itself.

At the end of a run, the transmission and time data are stored in a spreadsheet for further analysis. Although we have not worked on these possibilities, the system clearly has potential for applications to more exotic kinetic systems such as metabolic waves *(14),* or chaotic reaction systems *(7).*

Example 5 details.
There are many examples of published images similar to those of Figures 6 and 9, including photographic images of bright-line and dark-line spectra for gaseous atoms and molecules. It is obvious that such images can be recorded with a camera and then analysed by techniques very similar to those used here. Figure 12, reproduced in color below, represents a variation wherein an intensity "filter" is used to capture a subset of points. All that is required initially is to capture the (x,y) positions corresponding to pixel intensity values within a prescribed window, a straighforward programming problem in any language. In this example, positions of the oscilloscope grid were also used to check the linearity of the time and percent transmission scales in the image, and these could be used for

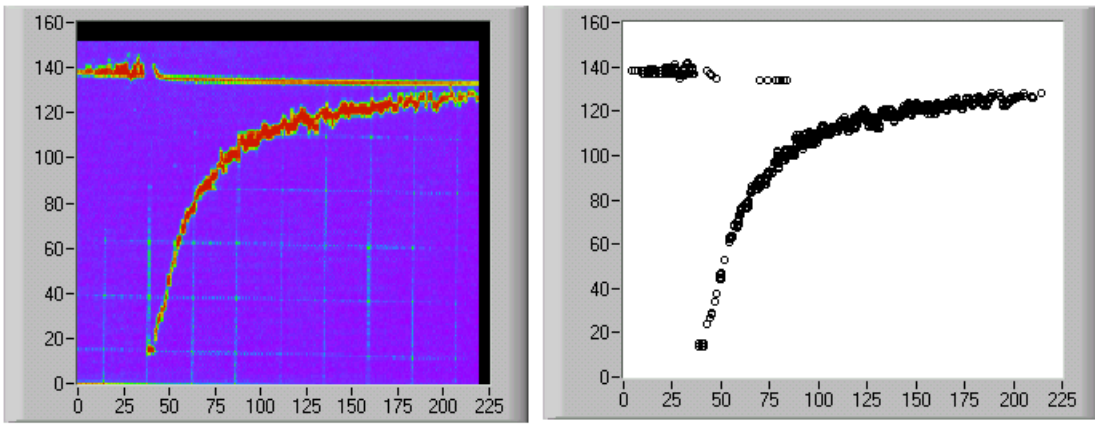

Figure 12 in color

image recalibration if necessary. Figure 19 below shows a second-order plot of the absorbance data retrieved from the image. The potential advantage of reprocessing is that many more points can be recovered than were used in the study of *(9),* where points were read from a Polaroid photo by hand. Another advantage is that digital smoothing might be used to remove some of the instrumental oscillation which becomes prominent at long times. For our purposes, it is sufficient to note that the slope of the Figure 19 graph for points later than 50 μs is very close to the published value. At earlier times, the reaction kinetics are considerably more complex. The slope in this example is related to the rate constant for the HCO bimolecular reaction by: $slope = 2k / \varepsilon l$ where ε is the HCO molar absorbtivity at 230 nm, and l is the sample path length, 20 cm in this example.

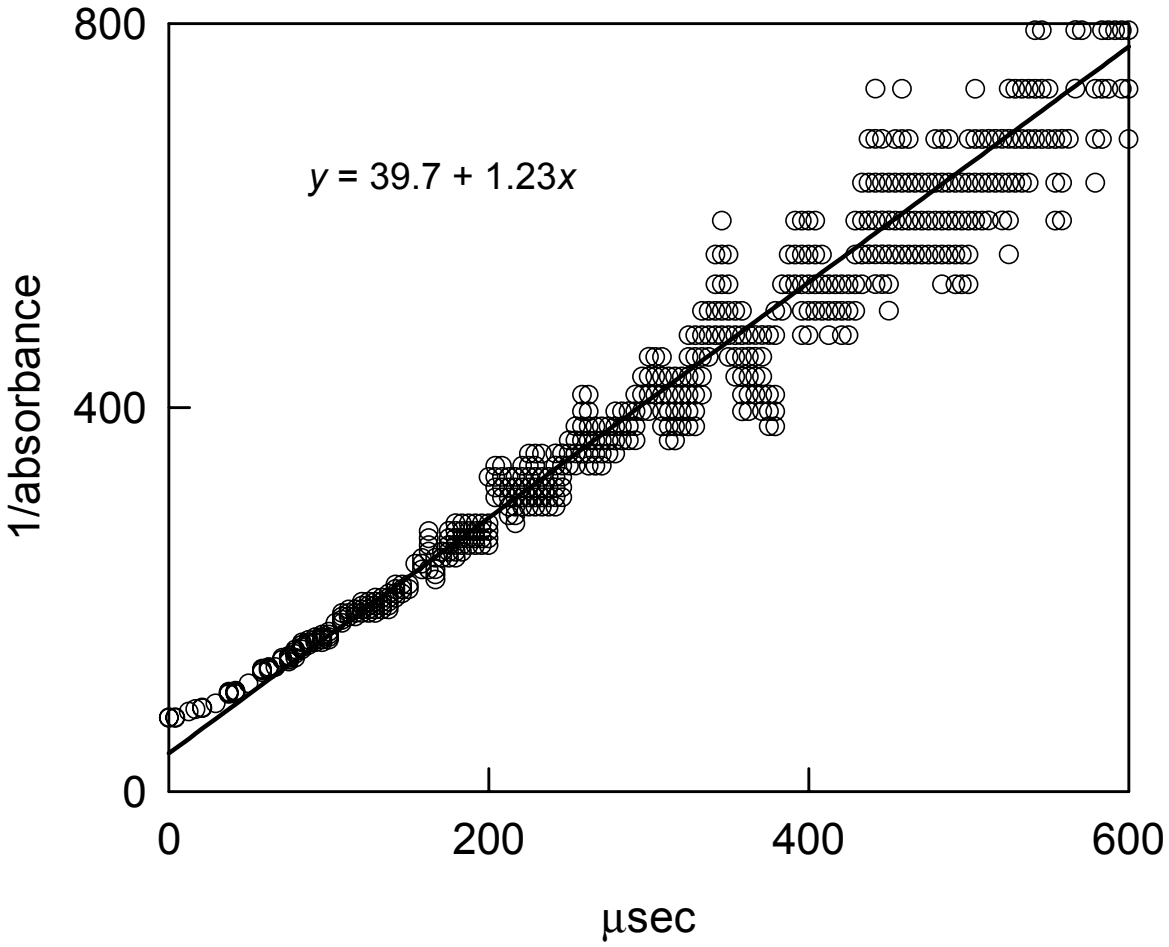

Figure 19

Additional References

10. Younger, M.S. *A Handbook for Linear Regres*sion, 1979, Wadsworth, California, Ch. 10.

11. Bevington, P.R.; Robinson D.K. *Data Reduction and Error Analysis for the Physical Sciences*, 2nd ed.; McGraw Hill:New York, 1993.

12. Hessler, J.P., *Int. J. Chem. Kinet*. **1997**, *29*, 803-817.

13. Tran, Y.; Whitten, J.E. *J. Chem. Educ*., **2001**, *78*, 1093-1095.

14. H.R. Petty, A.L. Kindzelskii, *J. Phys. Chem*. *B*, **2000**, *104*, 10952-10955.